

Recovering PCA from Hybrid- (ℓ_1, ℓ_2) Sparse Sampling of Data Elements

Abhisek Kundu *

Petros Drineas †

Malik Magdon-Ismail ‡

Abstract

This paper addresses how well we can recover a data matrix when only given a few of its elements. We present a randomized algorithm that element-wise sparsifies the data, retaining only a few its elements. Our new algorithm independently samples the data using sampling probabilities that depend on both the squares (ℓ_2 sampling) and absolute values (ℓ_1 sampling) of the entries. We prove that the hybrid algorithm recovers a near-PCA reconstruction of the data from a sublinear sample-size: hybrid- (ℓ_1, ℓ_2) inherits the ℓ_2 -ability to sample the important elements as well as the regularization properties of ℓ_1 sampling, and gives strictly better performance than either ℓ_1 or ℓ_2 on their own. We also give a one-pass version of our algorithm and show experiments to corroborate the theory.

1 Introduction

We address the problem of recovering a near-PCA reconstruction of the data from just a few of its entries – element-wise matrix sparsification (Achlioptas and McSherry (2001, 2007)). Read: you have a small sample of data points and those data points have missing features. This is a situation that one is confronted with all too often in machine learning. For example, with user-recommendation data, one does not have all the ratings of any given user. Or in a privacy preserving setting, a client may not want to give you all entries in the data matrix. In such a setting, our goal is to show that if the samples that you do get are chosen carefully, the top- k PCA features of the data can be recovered within some provable error bounds.

More formally, the data matrix is $\mathbf{A} \in \mathbb{R}^{m \times n}$ (m data points in n dimensions). Often, real data matrices have low effective rank, so let \mathbf{A}_k be the best rank- k approximation to \mathbf{A} with $\|\mathbf{A} - \mathbf{A}_k\|_2$ being small. \mathbf{A}_k is obtained by projecting \mathbf{A} onto the subspace spanned by its top- k principal components. In order to approximate this top- k principal subspace, we adopt the following strategy. Select a small number, s , of elements from \mathbf{A} and produce a sparse sketch $\tilde{\mathbf{A}}$; use the sparse sketch $\tilde{\mathbf{A}}$ to approximate the top- k singular subspace. In Section 4, we give the details of the algorithm and the theoretical guarantees on how well we recover the top- k principal subspace. The key quantity that one must control to recover a close approximation to PCA is how well the sparse sketch approximates the data *in the operator norm*. That is, if $\|\mathbf{A} - \tilde{\mathbf{A}}\|_2$ is small then you can recover PCA effectively.

Problem: sparse sampling of data elements

Given $\mathbf{A} \in \mathbb{R}^{m \times n}$ and $\epsilon > 0$, sample a small number of elements s to obtain a sparse sketch $\tilde{\mathbf{A}}$ for which

$$\|\mathbf{A} - \tilde{\mathbf{A}}\|_2 \leq \epsilon \quad \text{and} \quad \|\tilde{\mathbf{A}}\|_0 \leq s. \quad (1)$$

*Department of Computer Science, Rensselaer Polytechnic Institute, Troy, NY, kundua2@rpi.edu.

†Department of Computer Science, Rensselaer Polytechnic Institute, Troy, NY, drinep@cs.rpi.edu.

‡Department of Computer Science, Rensselaer Polytechnic Institute, Troy, NY, magdon@cs.rpi.edu.

Our main result addresses the problem above. In a nutshell, with only partially observed data that have been carefully selected, one can recover an approximation to the top- k principal subspace. An additional benefit is that computing our approximation to the top- k subspace using iterated multiplication can benefit computationally from sparsity. To construct $\tilde{\mathbf{A}}$, we use a general randomized approach which independently samples (and rescales) s elements from \mathbf{A} using probability p_{ij} to sample element \mathbf{A}_{ij} . We analyze in detail the case $p_{ij} \propto \alpha |\mathbf{A}_{ij}| + (1 - \alpha) |\mathbf{A}_{ij}|^2$ to get a bound on $\|\mathbf{A} - \tilde{\mathbf{A}}\|_2$. We now make our discussion precise, starting with our notation.

1.1 Notation

We use bold uppercase (e.g., \mathbf{X}) for matrices and bold lowercase (e.g., \mathbf{x}) for column vectors. The i -th row of \mathbf{X} is $\mathbf{X}_{(i)}$, and the i -th column of \mathbf{X} is $\mathbf{X}^{(i)}$. Let $[n]$ denote the set $\{1, 2, \dots, n\}$. $\mathbb{E}(X)$ is the expectation of a random variable X ; for a matrix, $\mathbb{E}(\mathbf{X})$ denotes the element-wise expectation. For a matrix $\mathbf{X} \in \mathbb{R}^{m \times n}$, the Frobenius norm $\|\mathbf{X}\|_F$ is $\|\mathbf{X}\|_F^2 = \sum_{i,j=1}^{m,n} \mathbf{X}_{ij}^2$, and the spectral (operator) norm $\|\mathbf{X}\|_2$ is $\|\mathbf{X}\|_2 = \max_{\|\mathbf{y}\|_2=1} \|\mathbf{X}\mathbf{y}\|_2$. We also have the ℓ_1 and ℓ_0 norms: $\|\mathbf{X}\|_1 = \sum_{i,j=1}^{m,n} |\mathbf{X}_{ij}|$ and $\|\mathbf{X}\|_0$ (the number of non-zero entries in \mathbf{X}). The k -th largest singular value of \mathbf{X} is $\sigma_k(\mathbf{X})$. For symmetric matrices \mathbf{X} , \mathbf{Y} , $\mathbf{Y} \succeq \mathbf{X}$ if and only if $\mathbf{Y} - \mathbf{X}$ is positive semi-definite. \mathbf{I}_n is the $n \times n$ identity and $\ln x$ is the natural logarithm of x . We use \mathbf{e}_i to denote standard basis vectors whose dimensions will be clear from the context.

Two popular sampling schemes are ℓ_1 ($p_{ij} = |\mathbf{A}_{ij}| / \|\mathbf{A}\|_1$ Achlioptas and McSherry (2001); Achlioptas et al. (2013)) and ℓ_2 ($p_{ij} = \mathbf{A}_{ij}^2 / \|\mathbf{A}\|_F^2$ Achlioptas and McSherry (2001); Drineas and Zouzias (2011)). We construct $\tilde{\mathbf{A}}$ as follows: $\tilde{\mathbf{A}}_{ij} = 0$ if the (i, j) -th entry is not sampled; sampled elements \mathbf{A}_{ij} are rescaled to $\tilde{\mathbf{A}}_{ij} = \mathbf{A}_{ij} / p_{ij}$ which makes the sketch $\tilde{\mathbf{A}}$ an unbiased estimator of \mathbf{A} , so $\mathbb{E}[\tilde{\mathbf{A}}] = \mathbf{A}$. The sketch is *sparse* if the number of sampled elements is sublinear, $s = o(mn)$. Sampling according to element magnitudes is natural in many applications, for example in a recommendation system users tend to rate a product they either like (high positive) or dislike (high negative).

Our main sparsification algorithm (Algorithm 1) receives as input a matrix \mathbf{A} and an accuracy parameter $\epsilon > 0$, and samples s elements from \mathbf{A} in s independent, identically distributed trials with replacement, according to a hybrid- (ℓ_1, ℓ_2) probability distribution specified in equation (2). The algorithm returns $\tilde{\mathbf{A}} \in \mathbb{R}^{m \times n}$, a sparse and unbiased estimator of \mathbf{A} , as a solution to (1).

1.2 Prior work

Achlioptas and McSherry (2001, 2007) pioneered the idea of ℓ_2 sampling for element-wise sparsification. However, ℓ_2 sampling on its own is not enough for provably accurate bounds for $\|\mathbf{A} - \tilde{\mathbf{A}}\|_2$. As a matter of fact Achlioptas and McSherry (2001, 2007) observed that “small” entries need to be sampled with probabilities that depend on their absolute values only, thus also introducing the notion of ℓ_1 sampling. The underlying reason for the need of ℓ_1 sampling is the fact that if a small element is sampled and rescaled using ℓ_2 sampling, this would result in a huge entry in $\tilde{\mathbf{A}}$ (because of the rescaling). As a result, the variance of ℓ_2 sampling is quite high, resulting in poor theoretical and experimental behavior. ℓ_1 sampling of small entries rectifies this issue by reducing the variance of the overall approach.

Arora et al. (2006) proposed a sparsification algorithm that deterministically keeps large entries, i.e., entries of \mathbf{A} such that $|\mathbf{A}_{ij}| \geq \epsilon / \sqrt{n}$ and randomly rounds the remaining entries using ℓ_1 sampling. Formally, entries of \mathbf{A} that are smaller than ϵ / \sqrt{n} are set to $\text{sign}(\mathbf{A}_{ij}) \epsilon / \sqrt{n}$ with probability $p_{ij} = \sqrt{n} |\mathbf{A}_{ij}| / \epsilon$ and to zero otherwise. They used an ϵ -net argument to show that $\|\mathbf{A} - \tilde{\mathbf{A}}\|_2$ was bounded with high probability. Drineas and Zouzias (2011) bypassed the need for ℓ_1 sampling by zeroing-out the small entries of \mathbf{A} (e.g., all entries such that $|\mathbf{A}_{ij}| < \epsilon / 2n$ for a matrix $\mathbf{A} \in \mathbb{R}^{n \times n}$) and then use ℓ_2 sampling on the remaining entries in order to sparsify the matrix. This simple modification improves Achlioptas and McSherry (2007) and Arora et al. (2006), and comes with an elegant proof using the matrix-Bernstein inequality

of Recht (2011). Note that all these approaches need truncation of small entries. Recently, Achlioptas et al. (2013) showed that ℓ_1 sampling in isolation could be done without any truncation, and argued that (under certain assumptions) ℓ_1 sampling would be better than ℓ_2 sampling, even using the truncation. Their proof is also based on the matrix-valued Bernstein inequality of Recht (2011).

1.3 Our Contributions

We introduce an intuitive hybrid approach to element-wise matrix sparsification, by combining ℓ_1 and ℓ_2 sampling. We propose to use sampling probabilities of the form

$$p_{ij} = \alpha \cdot \frac{|\mathbf{A}_{ij}|}{\|\mathbf{A}\|_1} + (1 - \alpha) \frac{\mathbf{A}_{ij}^2}{\|\mathbf{A}\|_F^2}, \quad \alpha \in (0, 1] \quad (2)$$

for all i, j ¹. We essentially retain the good properties of ℓ_2 sampling that bias us towards data elements in the presence of small noise, while *regularizing* smaller entries using ℓ_1 sampling. The proof of the quality-of-approximation result of Algorithm 1 (i.e. Theorem 1) uses the matrix-Bernstein Lemma 1. We summarize the main contributions below:

- We give a parameterized sampling distribution in the variable $\alpha \in (0, 1]$ that controls the balance between ℓ_2 sampling and ℓ_1 regularization. This greater flexibility allows us to achieve greater accuracy.
- We derive the optimal hybrid- (ℓ_1, ℓ_2) distribution, using Lemma 1 for arbitrary \mathbf{A} , by computing the optimal parameter α^* which produces the desired accuracy with smallest sample size according to our theoretical bound.

Our result generalizes the existing results because setting $\alpha = 1$ in our bounds reproduces the result of Achlioptas et al. (2013) who claim that ℓ_1 sampling is almost always better than ℓ_2 sampling. Our results show that $\alpha^* < 1$ which means that the hybrid approach is best.

- We give a provable algorithm (Algorithm 2) to implement hybrid- (ℓ_1, ℓ_2) sampling without knowing α *a priori*, i.e., we need not ‘fix’ the distribution using some predetermined value of α at the beginning of the sampling process. We can set α at a later stage, yet we can realize hybrid- (ℓ_1, ℓ_2) sampling. We use Algorithm 2 to propose a pass-efficient element-wise sampling model using only one pass over the elements of the data \mathbf{A} , using $O(s)$ memory. Moreover, Algorithm 3 gives us a heuristic to estimate α^* in one-pass over the data using $O(s)$ memory.

- Finally, we propose the Algorithm 4 which provably recovers PCA by constructing a sparse unbiased estimator of (centered) data using our optimal hybrid- (ℓ_1, ℓ_2) sampling.

Experimental results suggest that our optimal hybrid distribution (using α^*) requires strictly smaller sample size than ℓ_1 and ℓ_2 sampling (with or without truncation) to solve (1). Also, we achieve significant speed up of PCA on sparsified synthetic and real data while maintaining high quality approximation.

1.3.1 A Motivating Example for Hybrid- (ℓ_1, ℓ_2) Sampling

The main motivation for introducing the idea of hybrid- (ℓ_1, ℓ_2) sampling on elements of \mathbf{A} comes from achieving a tighter bound on s using a simple and intuitive probability distribution on elements of \mathbf{A} . For this, we observe certain good properties of both ℓ_1 and ℓ_2 sampling for sparsification of noisy data (in practice, we experience data that are noisy, and it is perhaps impossible to separate “true” data from noise). We illustrate the behavior of ℓ_1 and ℓ_2 sampling on noisy data using the following synthetic example. We construct a 500×500 binary data \mathbf{D} (Figure 1), and then perturb it by a random Gaussian matrix \mathbf{N} whose elements \mathbf{N}_{ij} follow Gaussian distribution with mean zero and standard deviation 0.1. We denote this perturbed data matrix by $\mathbf{A}_{0.1}$. First, we note that ℓ_1 and ℓ_2 sampling work *identically* on binary data \mathbf{D} .

¹combining ℓ_1 and ℓ_2 probabilities to avoid zeroing out step of ℓ_2 sampling has recently been observed by Kundu and Drineas (2014).

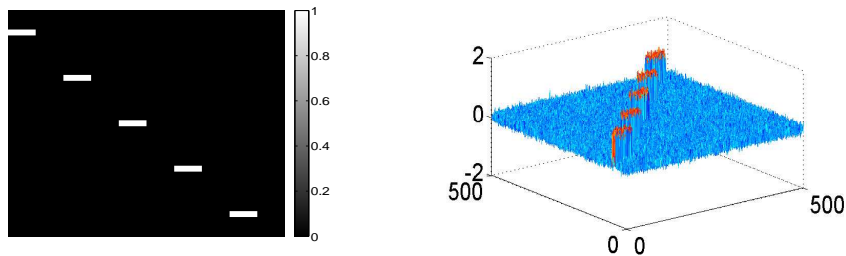


Figure 1: (left) Synthetic noiseless 500×500 binary data \mathbf{D} ; (right) mesh view of noisy data $\mathbf{A}_{0.1}$.

However, Figure 2 depicts the change in behavior of ℓ_1 and ℓ_2 sampling sparsifying $\mathbf{A}_{0.1}$. Data elements and noise in $\mathbf{A}_{0.1}$ are the elements with non-zero and zero values in \mathbf{D} , respectively. We sample $s = 5000$ indices in i.i.d. trials according to ℓ_1 and ℓ_2 probabilities separately to produce sparse sketch $\tilde{\mathbf{A}}$. Figure 2 shows that elements of $\tilde{\mathbf{A}}$, produced by ℓ_1 sampling, have controlled variance but most of them are noise. On the other hand, ℓ_2 sampling is biased towards data elements, although small number of sampled noisy elements create large variance due to rescaling. Our hybrid- (ℓ_1, ℓ_2) sampling benefits from this bias of ℓ_2 towards data elements, as well as, regularization properties of ℓ_1 .

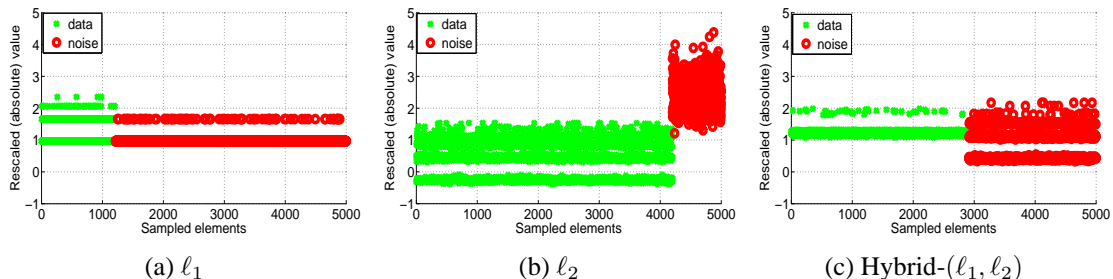


Figure 2: Elements of sparse sketch $\tilde{\mathbf{A}}$ produced from $\mathbf{A}_{0.1}$ via (a) ℓ_1 sampling, (b) ℓ_2 sampling, and (c) hybrid- (ℓ_1, ℓ_2) sampling with $\alpha = 0.7$. The y -axis plots the rescaled absolute values (in \ln scale) of $\tilde{\mathbf{A}}$ corresponding to the sampled indices. ℓ_1 sampling produces elements with controlled variance but it mostly samples noise, whereas ℓ_2 samples a lot of data although producing large variance of rescaled elements. Hybrid- (ℓ_1, ℓ_2) sampling uses ℓ_1 as a regularizer while sampling a fairly large number of data that helps to preserve the structure of original data.

We parameterize our distribution using the variable $\alpha \in (0, 1]$ that controls the balance between ℓ_2 sampling and ℓ_1 regularization. We derive an expression to compute α^* , the optimal α , corresponding to the smallest sample size that we need in order to achieve a given accuracy ϵ in (1). Setting $\alpha = 1$, we reproduce the result of Achlioptas et al. (2013). However, α^* may be smaller than 1, and the bound on sample size s , using α^* , is guaranteed to be tighter than that of Achlioptas et al. (2013).

2 Main Result

We present the quality-of-approximation result of our main algorithm (Algorithm 1). We define the sampling operator $\mathcal{S}_\Omega : \mathbb{R}^{m \times n} \rightarrow \mathbb{R}^{m \times n}$ in (3) that extracts elements from a given matrix $\mathbf{A} \in \mathbb{R}^{m \times n}$. Let Ω be a multi-set of sampled indices (i_t, j_t) , for $t = 1, \dots, s$. Then,

$$\mathcal{S}_\Omega(\mathbf{A}) = \frac{1}{s} \sum_{t=1}^s \frac{\mathbf{A}_{i_t j_t}}{p_{i_t j_t}} \mathbf{e}_{i_t} \mathbf{e}_{j_t}^T, \quad (i_t, j_t) \in \Omega \quad (3)$$

Algorithm 1 randomly samples (in i.i.d. trials) s elements of a given matrix \mathbf{A} , according to a probability distribution $\{p_{ij}\}_{i,j=1}^{m,n}$ over the elements of \mathbf{A} . Let the p_{ij} 's be as in eqn. (2). Then, we can prove the following theorem.

Theorem 1 *Let $\mathbf{A} \in \mathbb{R}^{m \times n}$ and let $\epsilon > 0$ be an accuracy parameter. Let \mathcal{S}_Ω be the sampling operator defined in (3), and assume that the multi-set Ω is generated using sampling probabilities $\{p_{ij}\}_{i,j=1}^{m,n}$ as in (2). Then, with probability at least $1 - \delta$,*

$$\|\mathcal{S}_\Omega(\mathbf{A}) - \mathbf{A}\|_2 \leq \epsilon \|\mathbf{A}\|_2, \quad (4)$$

if

$$s \geq \frac{2}{\epsilon^2 \|\mathbf{A}\|_2^2} (\rho^2(\alpha) + \gamma(\alpha)\epsilon \|\mathbf{A}\|_2 / 3) \ln \left(\frac{m+n}{\delta} \right) \quad (5)$$

where,

$$\xi_{ij} = \|\mathbf{A}\|_F^2 / \left(\frac{\alpha \cdot \|\mathbf{A}\|_F^2}{|\mathbf{A}_{ij}| \cdot \|\mathbf{A}\|_1} + (1 - \alpha) \right), \text{ for } \mathbf{A}_{ij} \neq 0,$$

$$\rho^2(\alpha) = \max \left\{ \max_i \sum_{j=1}^n \xi_{ij}, \max_j \sum_{i=1}^m \xi_{ij} \right\} - \sigma_{\min}^2(\mathbf{A}),$$

$$\gamma(\alpha) = \max_{\substack{i,j: \\ \mathbf{A}_{ij} \neq 0}} \left\{ \frac{\|\mathbf{A}\|_1}{\alpha + (1 - \alpha) \frac{\|\mathbf{A}\|_1 \cdot |\mathbf{A}_{ij}|}{\|\mathbf{A}\|_F^2}} \right\} + \|\mathbf{A}\|_2,$$

$\sigma_{\min}(\mathbf{A})$ is the smallest singular value of \mathbf{A} . Moreover, we can find α^* (optimal α corresponding to the smallest s) and s^* (the smallest s), by solving the following optimization problem in (6):

$$\alpha^* = \min_{\alpha \in (0,1]} f(\alpha), \quad f(\alpha) = \rho^2(\alpha) + \gamma(\alpha)\epsilon \|\mathbf{A}\|_2 / 3, \quad (6)$$

$$s^* = \frac{2}{\epsilon^2 \|\mathbf{A}\|_2^2} \left(\rho^2(\alpha^*) + \gamma(\alpha^*) \frac{\epsilon \|\mathbf{A}\|_2}{3} \right) \ln \left(\frac{m+n}{\delta} \right) \quad (7)$$

The functional form in (5) comes from the Matrix-Bernstein inequality in Lemma 1, with ρ^2 and γ being functions of \mathbf{A} and α . This gives us a flexibility to optimize the sample size with respect to α in (5), which is how we get the optimal α^* . For a given matrix \mathbf{A} , we can easily compute $\rho^2(\alpha)$ and $\gamma(\alpha)$ for various values of α . Given an accuracy ϵ and failure probability δ , we can compute α^* corresponding to the tightest bound on s . Note that, for $\alpha = 1$ we reproduce the results of Achlioptas et al. (2013) (which was expressed using various matrix metrics). However, α^* may be smaller than 1, and is guaranteed to produce tighter s comparing to extreme choices of α (e.g. $\alpha = 1$ for ℓ_1 sampling). We illustrate this by the plot in Figure 3. We give a proof of Theorem 1 in Section 2.1.

2.1 Proof of Theorem 1

In this section we provide a proof of Theorem 1 following the proof outline of Drineas and Zouzias (2011); Achlioptas et al. (2013). We use the following non-commutative matrix-valued Bernstein bound of Recht (2011) as our main tool to prove Theorem 1. Using our notation we rephrase the matrix Bernstein bound.

Algorithm 1 Element-wise Matrix Sparsification

- 1: **Input:** $\mathbf{A} \in \mathbb{R}^{m \times n}$, accuracy parameter $\epsilon > 0$.
 - 2: **Set** s as in eq. (7).
 - 3: **For** $t = 1 \dots s$ (i.i.d. trials with replacement) **randomly sample** pairs of indices $(i_t, j_t) \in [m] \times [n]$ with $\mathbb{P}[(i_t, j_t) = (i, j)] = p_{ij}$, where p_{ij} are as in (2), using α as in (6).
 - 4: **Output**(sparse): $\mathcal{S}_\Omega(\mathbf{A}) = \frac{1}{s} \sum_{t=1}^s \frac{\mathbf{A}_{i_t j_t}}{p_{i_t j_t}} \mathbf{e}_{i_t} \mathbf{e}_{j_t}^T$.
-

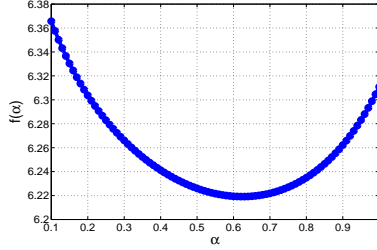


Figure 3: Plot of $f(\alpha)$ in eqn (6) for data $\mathbf{A}_{0.1}$. We use $\epsilon = 0.05$ and $\delta = 0.1$. x -axis plots α and y -axis is in \log_{10} scale. For this data, $\alpha^* \approx 0.6$.

Lemma 1 [Theorem 3.2 of Recht (2011)] Let $\mathbf{M}_1, \mathbf{M}_2, \dots, \mathbf{M}_s$ be independent, zero-mean random matrices in $\mathbb{R}^{m \times n}$. Suppose

$$\max_{t \in [s]} \{ \|\mathbb{E}(\mathbf{M}_t \mathbf{M}_t^T)\|_2, \|\mathbb{E}(\mathbf{M}_t^T \mathbf{M}_t)\|_2 \} \leq \rho^2$$

and $\|\mathbf{M}_t\|_2 \leq \gamma$ for all $t \in [s]$. Then, for any $\epsilon > 0$,

$$\left\| \frac{1}{s} \sum_{t=1}^s \mathbf{M}_t \right\|_2 \leq \epsilon$$

holds, subject to a failure probability at most

$$(m+n) \exp\left(\frac{-s\epsilon^2/2}{\rho^2 + \gamma\epsilon/3}\right).$$

For all $t \in [s]$ we define the matrix $\mathbf{M}_t \in \mathbb{R}^{m \times n}$ as follows:

$$\mathbf{M}_t = \frac{\mathbf{A}_{i_t j_t}}{p_{i_t j_t}} \mathbf{e}_{i_t} \mathbf{e}_{j_t}^T - \mathbf{A}.$$

It now follows that

$$\frac{1}{s} \sum_{t=1}^s \mathbf{M}_t = \frac{1}{s} \sum_{t=1}^s \left[\frac{\mathbf{A}_{i_t j_t}}{p_{i_t j_t}} \mathbf{e}_{i_t} \mathbf{e}_{j_t}^T - \mathbf{A} \right] = \mathcal{S}_\Omega(\mathbf{A}) - \mathbf{A}.$$

We can bound $\|\mathbf{M}_t\|_2$ for all $t \in [s]$. We define the following quantity:

$$\lambda = \frac{\|\mathbf{A}\|_1 \cdot |\mathbf{A}_{ij}|}{\|\mathbf{A}\|_F^2}, \text{ for } \mathbf{A}_{ij} \neq 0 \quad (8)$$

Lemma 2 Using our notation, and using probabilities of the form (2), for all $t \in [s]$,

$$\|\mathbf{M}_t\|_2 \leq \max_{\substack{i,j: \\ \mathbf{A}_{ij} \neq 0}} \frac{\|\mathbf{A}\|_1}{\alpha + (1-\alpha)\lambda} + \|\mathbf{A}\|_2.$$

Proof: Using probabilities of the form (2), and because $\mathbf{A}_{ij} = 0$ is never sampled,

$$\|\mathbf{M}_t\|_2 = \left\| \frac{\mathbf{A}_{i_t j_t} \mathbf{e}_{i_t} \mathbf{e}_{j_t}^T}{p_{i_t j_t}} - \mathbf{A} \right\|_2 \leq \max_{\substack{i,j: \\ \mathbf{A}_{ij} \neq 0}} \left\{ \left(\frac{\alpha}{\|\mathbf{A}\|_1} + \frac{(1-\alpha) \cdot |\mathbf{A}_{ij}|}{\|\mathbf{A}\|_F^2} \right)^{-1} \right\} + \|\mathbf{A}\|_2$$

Using (8), we obtain the bound. ◇

Next we bound the spectral norm of the expectation of $\mathbf{M}_t \mathbf{M}_t^T$.

Lemma 3 *Using our notation, and using probabilities of the form (2), for all $t \in [s]$,*

$$\|\mathbb{E}[\mathbf{M}_t \mathbf{M}_t^T]\|_2 \leq \|\mathbf{A}\|_F^2 \beta_1 - \sigma_{\min}^2(\mathbf{A}),$$

where,

$$\beta_1 = \max_i \sum_{j=1}^n \left(\frac{\alpha \cdot \|\mathbf{A}\|_F^2}{|\mathbf{A}_{ij}| \cdot \|\mathbf{A}\|_1} + (1-\alpha) \right)^{-1}, \text{ for } \mathbf{A}_{ij} \neq 0.$$

Proof: Recall that $\mathbf{A} = \sum_{i,j=1}^{m,n} \mathbf{A}_{ij} \mathbf{e}_i \mathbf{e}_j^T$ and $\mathbf{M}_t = \frac{\mathbf{A}_{i_t j_t} \mathbf{e}_{i_t} \mathbf{e}_{j_t}^T}{p_{i_t j_t}} - \mathbf{A}$ to derive

$$\begin{aligned} \mathbb{E}[\mathbf{M}_t \mathbf{M}_t^T] &= \sum_{i,j=1}^{m,n} p_{ij} \left(\frac{\mathbf{A}_{ij} \mathbf{e}_i \mathbf{e}_j^T}{p_{ij}} - \mathbf{A} \right) \left(\frac{\mathbf{A}_{ij} \mathbf{e}_j \mathbf{e}_i^T}{p_{ij}} - \mathbf{A}^T \right) \\ &= \sum_{i,j=1}^{m,n} \left(\frac{\mathbf{A}_{ij}^2 \mathbf{e}_i \mathbf{e}_i^T}{p_{ij}} \right) - \mathbf{A} \mathbf{A}^T. \end{aligned}$$

Sampling according to probabilities of eqn. (2), and because $\mathbf{A}_{ij} = 0$ is never sampled, we get, for $\mathbf{A}_{ij} \neq 0$,

$$\begin{aligned} \sum_{i,j=1}^{m,n} \frac{\mathbf{A}_{ij}^2}{p_{ij}} &= \|\mathbf{A}\|_F^2 \sum_{i,j=1}^{m,n} \left(\frac{\alpha \cdot \|\mathbf{A}\|_F^2}{|\mathbf{A}_{ij}| \cdot \|\mathbf{A}\|_1} + (1-\alpha) \right)^{-1}, \\ &\leq \|\mathbf{A}\|_F^2 \sum_{i=1}^m \max_i \sum_{j=1}^n \left(\frac{\alpha \cdot \|\mathbf{A}\|_F^2}{|\mathbf{A}_{ij}| \cdot \|\mathbf{A}\|_1} + (1-\alpha) \right)^{-1}. \end{aligned}$$

Thus,

$$\mathbb{E}[\mathbf{M}_t \mathbf{M}_t^T] \preceq \|\mathbf{A}\|_F^2 \beta_1 \sum_{i=1}^m \mathbf{e}_i \mathbf{e}_i^T - \mathbf{A} \mathbf{A}^T = \|\mathbf{A}\|_F^2 \beta_1 \mathbf{I}_m - \mathbf{A} \mathbf{A}^T.$$

Note that, $\|\mathbf{A}\|_F^2 \beta_1 \mathbf{I}_m$ is a diagonal matrix with all entries non-negative, and $\mathbf{A} \mathbf{A}^T$ is a positive semi-definite matrix. Therefore,

$$\|\mathbb{E}[\mathbf{M}_t \mathbf{M}_t^T]\|_2 \leq \|\mathbf{A}\|_F^2 \beta_1 - \sigma_{\min}^2(\mathbf{A}).$$

Similarly, we can obtain ◇

$$\|\mathbb{E}[\mathbf{M}_t^T \mathbf{M}_t]\|_2 \leq \|\mathbf{A}\|_F^2 \beta_2 - \sigma_{\min}^2(\mathbf{A}),$$

where,

$$\beta_2 = \max_j \sum_{i=1}^m \left(\frac{\alpha \cdot \|\mathbf{A}\|_F^2}{|\mathbf{A}_{ij}| \cdot \|\mathbf{A}\|_1} + (1 - \alpha) \right)^{-1}, \text{ for } \mathbf{A}_{ij} \neq 0.$$

We can now apply Theorem 1 with

$$\rho^2(\alpha) = \|\mathbf{A}\|_F^2 \max\{\beta_1, \beta_2\} - \sigma_{\min}^2(\mathbf{A})$$

and

$$\gamma(\alpha) = \frac{\|\mathbf{A}\|_1}{\alpha + (1 - \alpha)\lambda} + \|\mathbf{A}\|_2$$

to conclude that $\|\mathcal{S}_\Omega(\mathbf{A}) - \mathbf{A}\|_2 \leq \varepsilon$ holds subject to a failure probability at most

$$(m + n) \exp((-s\varepsilon^2/2)/(\rho^2(\alpha) + \gamma(\alpha)\varepsilon/3)).$$

Bounding the failure probability by δ , and setting $\varepsilon = \epsilon \cdot \|\mathbf{A}\|_2$, we complete the proof.

3 One-pass Hybrid- (ℓ_1, ℓ_2) Sampling

Here we discuss the implementation of (ℓ_1, ℓ_2) -hybrid sampling in one pass over the input matrix \mathbf{A} using $O(s)$ memory, that is, a streaming model. We know that both ℓ_1 and ℓ_2 sampling can be done in one pass using $O(s)$ memory (see Algorithm SELECT p. 137 of Drineas et al. (2006)). In our hybrid sampling, we want parameter α to depend on data elements, i.e., we do not want to ‘fix’ it prior to the arrival of data stream. Here we give an algorithm (Algorithm 2) to implement a one-pass version of the hybrid sampling *without knowing α a priori*.

We note that steps 2-5 of Algorithm 2 access the elements of \mathbf{A} only once, in parallel, to form independent multisets S_1, S_2, S_3 , and S_4 . Step 6 computes $\|\mathbf{A}\|_F^2$ and $\|\mathbf{A}\|_1$ in parallel in one pass over \mathbf{A} . Subsequent steps do not need to access \mathbf{A} anymore. Interestingly, we set α in step 7 when the data stream is gone. Steps 10-16 sample s elements from S_1 and S_2 based on the α in step 7, and produce sparse matrix \mathbf{X} based on the sampled entries in random multiset S . Theorem 2 shows that Algorithm 2 indeed samples elements from \mathbf{A} according to the hybrid- (ℓ_1, ℓ_2) probabilities in eqn (2).

Theorem 2 *Using the notations in Algorithm 2, for $\alpha \in (0, 1]$, $t = 1, \dots, s$,*

$$P[S(t) = (i, j, \mathbf{A}_{ij})] = \alpha \cdot p_1 + (1 - \alpha) \cdot p_2,$$

where $p_1 = \frac{|\mathbf{A}_{ij}|}{\|\mathbf{A}\|_1}$ and $p_2 = \frac{\mathbf{A}_{ij}^2}{\|\mathbf{A}\|_F^2}$.

Proof: Here we use the notations in Theorem 2. Note that t -th elements of S_1 and S_2 are sampled independently with ℓ_1 and ℓ_2 probabilities, respectively. We consider the following disjoint events:

$$\mathcal{E}_1 : S_1(t) = (i, j, \mathbf{A}_{ij}) \wedge S_2(t) \neq (i, j, \mathbf{A}_{ij})$$

$$\mathcal{E}_2 : S_1(t) \neq (i, j, \mathbf{A}_{ij}) \wedge S_2(t) = (i, j, \mathbf{A}_{ij})$$

$$\mathcal{E}_3 : S_1(t) = (i, j, \mathbf{A}_{ij}) \wedge S_2(t) = (i, j, \mathbf{A}_{ij})$$

$$\mathcal{E}_4 : S_1(t) \neq (i, j, \mathbf{A}_{ij}) \wedge S_2(t) \neq (i, j, \mathbf{A}_{ij})$$

Let us denote the events $x_1 : x \geq \alpha$ and $x_2 : x < \alpha$. Clearly, $P[x_1] = \alpha, P[x_2] = 1 - \alpha$. Since the elements $S_1(t)$ and $S_2(t)$ are sampled independently, we have

$$P[\mathcal{E}_1] = P[S_1(t) = (i, j, \mathbf{A}_{ij})]P[S_2(t) \neq (i, j, \mathbf{A}_{ij})] = p_1(1 - p_2)$$

$$P[\mathcal{E}_2] = (1 - p_1)p_2$$

$$P[\mathcal{E}_3] = p_1p_2$$

$$P[\mathcal{E}_4] = (1 - p_1)(1 - p_2)$$

Algorithm 2 One-pass hybrid- (ℓ_1, ℓ_2) sampling

- 1: **Input:** \mathbf{A}_{ij} for all $(i, j) \in [m] \times [n]$, arbitrarily ordered, and sample size s .
 - 2: Apply SELECT algorithm in parallel with $O(s)$ memory using ℓ_1 probabilities to sample s independent indices (i_{t_1}, j_{t_1}) and corresponding elements $\mathbf{A}_{i_{t_1}j_{t_1}}$ to form random multiset S_1 of triples $(i_{t_1}, j_{t_1}, \mathbf{A}_{i_{t_1}j_{t_1}})$, for $t_1 = 1, \dots, s$.
 - 3: Run step 2 in parallel to form another independent multiset S_3 of triples $(i_{t_3}, j_{t_3}, \mathbf{A}_{i_{t_3}j_{t_3}})$, for $t_3 = 1, \dots, s$. (This step is only for Algorithm 3)
 - 4: Apply SELECT algorithm in parallel with $O(s)$ memory using ℓ_2 probabilities to sample s independent indices (i_{t_2}, j_{t_2}) and corresponding elements $\mathbf{A}_{i_{t_2}j_{t_2}}$ to form random multiset S_2 of triples $(i_{t_2}, j_{t_2}, \mathbf{A}_{i_{t_2}j_{t_2}})$, for $t_2 = 1, \dots, s$.
 - 5: Run step 4 in parallel to form another independent multiset S_4 of triples $(i_{t_4}, j_{t_4}, \mathbf{A}_{i_{t_4}j_{t_4}})$, for $t_4 = 1, \dots, s$. (This step is only for Algorithm 3)
 - 6: Compute and store $\|\mathbf{A}\|_F^2$ and $\|\mathbf{A}\|_1$ in parallel.
 - 7: Set the value of $\alpha \in (0, 1]$ (using Algorithm 3).
 - 8: Create empty multiset of triples S .
 - 9: $\mathbf{X} \leftarrow \mathbf{0}_{m \times n}$.
 - 10: **For** $t = 1 \dots s$
 - 11: Generate a uniform random number $x \in [0, 1]$.
 - 12: if $x \geq \alpha$, $S(t) \leftarrow S_1(t)$; otherwise, $S(t) \leftarrow S_2(t)$.
 - 13: $(i_t, j_t) \leftarrow S(t, 1 : 2)$.
 - 14: $p \leftarrow \alpha \cdot \frac{|S(t,3)|}{\|\mathbf{A}\|_1} + (1 - \alpha) \cdot \frac{|S(t,3)|^2}{\|\mathbf{A}\|_F^2}$
 - 15: $\mathbf{X} \leftarrow \mathbf{X} + \frac{S(t,3)}{p \cdot s} e_{i_t} e_{j_t}^T$.
 - 16: **End**
 - 17: **Output:** random multiset S , and sparse matrix \mathbf{X} .
-

We note that α may be dependent on the elements of S_3 and S_4 (in Algorithm 3), but is independent of elements of S_1 and S_2 . Therefore, events x_1 and x_2 are independent of the events \mathcal{E}_j , $j = 1, 2, 3, 4$. Thus,

$$\begin{aligned}
 & P[S(t) = (i, j, \mathbf{A}_{ij})] \\
 &= P[(\mathcal{E}_1 \wedge x_1) \vee (\mathcal{E}_2 \wedge x_2) \vee \mathcal{E}_3] \\
 &= P[\mathcal{E}_1 \wedge x_1] + P[\mathcal{E}_2 \wedge x_2] + P[\mathcal{E}_3] \\
 &= P[\mathcal{E}_1]P[x_1] + P[\mathcal{E}_2]P[x_2] + P[\mathcal{E}_3] \\
 &= p_1(1 - p_2)\alpha + (1 - p_1)p_2(1 - \alpha) + p_1p_2 \\
 &= \alpha \cdot p_1 + (1 - \alpha) \cdot p_2
 \end{aligned}$$

◇

Note that, Theorem 2 holds for any arbitrary $\alpha \in (0, 1]$ in line 7 of Algorithm 2, i.e., Algorithm 3 is not essential for correctness of Theorem 2. We only need α to be independent of elements of S_1 and S_2 . However, we use Algorithm 3 to get an iterative estimate of α^* (Section 3.1) in one pass over \mathbf{A} . In this case, we need additional independent multisets S_3 and S_4 to ‘learn’ the parameter α^* . Algorithm 2 (without Algorithm 3) requires a memory twice as large required by ℓ_1 or ℓ_2 sampling. Using Algorithm 3 this requirement is four times as large. However, in both the cases the asymptotic memory requirement remains the same $O(s)$.

Algorithm 3 Iterative estimate of α^*

- 1: **Input:** Multiset of triples S_3 and S_4 with s elements each, number of iteration τ , accuracy ϵ , $\|\mathbf{A}\|_F^2$, and $\|\mathbf{A}\|_1$.
 - 2: Create empty multiset of triples S .
 - 3: $\alpha_0 = 0.5$
 - 4: **For** $k = 1 \dots \tau$
 - 5: $\mathbf{X} \leftarrow \mathbf{0}_{m \times n}$.
 - 6: **For** $t = 1 \dots s$
 - 7: Generate a uniform random number $x \in [0, 1]$.
 - 8: If $x \geq \alpha_{k-1}$, $S(t) \leftarrow S_3(t)$; else, $S(t) \leftarrow S_4(t)$.
 - 9: $(i_t, j_t) \leftarrow S(t, 1 : 2)$.
 - 10: $p \leftarrow \alpha_{k-1} \cdot \frac{|S(t,3)|}{\|\mathbf{A}\|_1} + (1 - \alpha_{k-1}) \cdot \frac{|S(t,3)|^2}{\|\mathbf{A}\|_F^2}$
 - 11: $\mathbf{X} \leftarrow \mathbf{X} + \frac{S(t,3)}{p \cdot s} e_{i_t} e_{j_t}^T$.
 - 12: **End**
 - 13: $\alpha_k \leftarrow \tilde{\alpha}$ in (9) using \mathbf{X} .
 - 14: **End**
 - 15: **Output:** α_τ .
-

3.1 Iterative Estimate of α^*

We obtain independent random multiset of triples S_3 and S_4 , each containing s elements from \mathbf{A} in one pass, in Algorithm 2. We can create a sparse random matrix \mathbf{X} , as shown in step 11 in Algorithm 3, that is an unbiased estimator of \mathbf{A} . We use this \mathbf{X} as a proxy for \mathbf{A} to estimate the quantities we need in order to solve the optimization problem in (9).

$$\tilde{\alpha} : \min_{\alpha \in (0,1)} \{ (\tilde{\rho}^2(\alpha) + \tilde{\gamma}(\alpha)\epsilon \|\mathbf{X}\|_2 / 3) \} \quad (9)$$

where, for all $(i, j) \in S(:, 1 : 2)$

$$\begin{aligned} \tilde{\xi}_{ij} &= \|\mathbf{X}\|_F^2 / \left(\frac{\alpha \cdot \|\mathbf{X}\|_F^2}{|\mathbf{X}_{ij}| \cdot \|\mathbf{X}\|_1} + (1 - \alpha) \right), \\ \tilde{\rho}^2(\alpha) &= \max \left\{ \max_i \sum_{j=1}^n \tilde{\xi}_{ij}, \max_j \sum_{i=1}^m \tilde{\xi}_{ij} \right\}, \\ \tilde{\gamma}(\alpha) &= \max_{ij} \left\{ \frac{\|\mathbf{X}\|_1}{\alpha + (1 - \alpha) \frac{\|\mathbf{X}\|_1 \cdot |\mathbf{X}_{ij}|}{\|\mathbf{X}\|_F^2}} \right\} + \|\mathbf{X}\|_F. \end{aligned}$$

We note that $\|\mathbf{X}\|_0 \leq s$. We can compute the quantities $\tilde{\rho}(\alpha)$ and $\tilde{\gamma}(\alpha)$, for a fixed α , using $O(s)$ memory. We consider $\varepsilon = \epsilon \cdot \|\mathbf{X}\|_2$ to be the given accuracy.

4 Fast Approximation of PCA

Here, we discuss a provable algorithm (Algorithm 4) to speed up computation of PCA applying element-wise sampling. We sparsify a given centered data \mathbf{A} to produce a sparse unbiased estimator $\tilde{\mathbf{A}}$ by sampling s elements in i.i.d. trials according to our hybrid- (ℓ_1, ℓ_2) distribution in (2). Computation of rank-truncated

Algorithm 4 Fast Approximation of PCA

- 1: **Input:** Centered data $\mathbf{A} \in \mathbb{R}^{m \times n}$, sparsity parameter $s > 0$, and rank parameter k .
 - 2: Produce sparse unbiased estimator $\tilde{\mathbf{A}}$ from \mathbf{A} , in s i.i.d. trials using Algorithm 1.
 - 3: Perform rank truncated SVD on sparse matrix $\tilde{\mathbf{A}}$, i.e., $[\tilde{\mathbf{U}}_k, \tilde{\mathbf{D}}_k, \tilde{\mathbf{V}}_k] = \text{SVD}(\tilde{\mathbf{A}}, k)$.
 - 4: **Output:** $\tilde{\mathbf{V}}_k$ (columns of $\tilde{\mathbf{V}}_k$ are the ordered PCA's).
-

SVD on sparse data is fast, and we consider the right singular vectors of $\tilde{\mathbf{A}}$ as the approximate principal components of \mathbf{A} . Naturally, more samples produce better approximation. However, this reduces sparsity, and consequently we lose the speed advantage. Theorem 3 shows the quality of approximation of principal components produced by Algorithm 4.

Theorem 3 *Let $\mathbf{A} \in \mathbb{R}^{m \times n}$ be a given matrix, and $\tilde{\mathbf{A}}$ be a sparse sketch produced by Algorithm 1. Let $\tilde{\mathbf{V}}_k$ be the PCA's of $\tilde{\mathbf{A}}$ computed in step 3 of Algorithm 4. Then*

$$\begin{aligned} \left\| \mathbf{A} - \mathbf{A} \tilde{\mathbf{V}}_k \tilde{\mathbf{V}}_k^T \right\|_F^2 &\leq \left\| \mathbf{A} - \mathbf{A}_k \right\|_F^2 + \frac{4 \left\| \mathbf{A}_k \right\|_F^2}{\sigma_k(\mathbf{A})} \left\| \mathbf{A} - \tilde{\mathbf{A}} \right\|_2 \\ \left\| \mathbf{A}_k - \tilde{\mathbf{A}}_k \right\|_F &\leq \sqrt{8k} \cdot \left(\left\| \mathbf{A} - \mathbf{A}_k \right\|_2 + \left\| \mathbf{A} - \tilde{\mathbf{A}} \right\|_2 \right) \\ \left\| \mathbf{A} - \tilde{\mathbf{A}}_k \right\|_F &\leq \left\| \mathbf{A} - \mathbf{A}_k \right\|_F + \sqrt{8k} \cdot \left(\left\| \mathbf{A} - \mathbf{A}_k \right\|_2 + \left\| \mathbf{A} - \tilde{\mathbf{A}} \right\|_2 \right) \end{aligned}$$

The first inequality of Theorem 3 bounds the approximation of projected data onto the space spanned by top k approximate PCA's. The second and third inequalities measure the quality of $\tilde{\mathbf{A}}_k$ as a surrogate for \mathbf{A}_k and the quality of projection of sparsified data onto approximate PCA's, respectively.

Proofs of first two inequalities of Theorem 3 follow from Theorem 5 and Theorem 8 of Achlioptas and McSherry (2001), respectively. The last inequality follows from the triangle inequality. The last two inequalities above are particularly useful in cases where \mathbf{A} is inherently low-rank and we choose an appropriate k for approximation, for which $\left\| \mathbf{A} - \mathbf{A}_k \right\|_2$ is small.

5 Experiments

In this section we perform various element-wise sampling experiments on synthetic and real data to show how well the sparse sketches preserve the structure of the original data, in spectral norm. Also, we show results on the quality of the PCA's derived from sparse sketches.

5.1 Algorithms for Sparse Sketches

We use Algorithm 1 as a prototypical algorithm to produce sparse sketches from a given matrix via various sampling methods. Note that, we can plug-in any element-wise probability distribution in Algorithm 1 to produce (unbiased) sparse matrices. We construct sparse sketches via our optimal hybrid- (ℓ_1, ℓ_2) sampling, along with other sampling methods related to extreme choices of α , such as, ℓ_1 sampling for $\alpha = 1$. Also, we use *element-wise leverage scores* (Chen et al. (2014)) for sparsification of *low-rank* data. Element-wise leverage scores are used in the context of *low-rank matrix completion* by Chen et al. (2014). Let \mathbf{A} be a $m \times n$ matrix of rank ρ , and its SVD if given by $\mathbf{A} = \mathbf{U}\Sigma\mathbf{V}^T$. Then, we define μ_i (row leverage scores), ν_j (column leverage scores), and element-wise leverage scores p_{lev} as follows:

$$\mu_i = \left\| \mathbf{U}_{(i)} \right\|_2^2, \quad \nu_j = \left\| \mathbf{V}_{(j)} \right\|_2^2, \quad p_{lev} = \frac{\mu_i + \nu_j}{(m+n)\rho}, \quad i \in [m], j \in [n]$$

Note that p_{lev} is a probability distribution on the elements of \mathbf{A} . Leverage scores become uniform if the matrix \mathbf{A} is full rank. We use p_{lev} in Algorithm 1 to produce sparse sketch $\tilde{\mathbf{A}}$ of a low-rank data \mathbf{A} .

5.1.1 Experimental Design for Sparse Sketches

We compute the theoretical optimal mixing parameter α^* by solving eqn (6) for various datasets. We compare this α^* with the theoretical condition derived by Achlioptas et al. (2013) (for cases when ℓ_1 sampling outperforms ℓ_2 sampling). We verify the accuracy of α^* by measuring the quality of the sparse sketches $\tilde{\mathbf{A}}$, $\mathcal{E} = \|\mathbf{A} - \tilde{\mathbf{A}}\|_2 / \|\mathbf{A}\|_2$ for various sampling distributions. Let \mathcal{E}_h , \mathcal{E}_1 , and \mathcal{E}_{lev} denote the quality of sparse sketches produced via optimal hybrid sampling, ℓ_1 sampling, and element-wise leverage scores p_{lev} , respectively. We compare \mathcal{E}_h , \mathcal{E}_1 , and \mathcal{E}_{lev} for various sample sizes for real and synthetic datasets.

5.2 Algorithms for Fast PCA

We compare three algorithms for computing PCA of the centered data. Let the actual PCA of the original data be \mathcal{A} . We use Algorithm 4 to compute approximate PCA via our optimal hybrid- (ℓ_1, ℓ_2) sampling. Let us denote this approximate PCA by \mathcal{H} . Also, we compute PCA of a Gaussian random projection of the original data to compare the quality of \mathcal{H} . Let $\mathbf{A}_G = \mathbf{G}\mathbf{A} \in \mathbb{R}^{r \times n}$, where $\mathbf{A} \in \mathbb{R}^{m \times n}$ is the original data, and \mathbf{G} is a $r \times m$ standard Gaussian matrix. Let the PCA of this random projection \mathbf{A}_G be \mathcal{G} . Also, let T_a, T_h , and T_G be the computation time (in milliseconds) for \mathcal{A} , \mathcal{H} , and \mathcal{G} , respectively.

5.2.1 Experimental Design for Fast PCA

We compare the visual quality of \mathcal{A} , \mathcal{H} , and \mathcal{G} for image datasets. Also, we compare the computation time T_a, T_h , and T_G for these datasets.

5.3 Description of Data

In this section we describe the synthetic and real datasets we use in our experiments.

5.3.1 Synthetic Data

We construct a binary 500×500 image data \mathbf{D} (see Figure 1). We add random noise to perturb the elements of the ‘pure’ data \mathbf{D} . Specifically, we construct a 500×500 noise matrix \mathbf{N} whose elements \mathbf{N}_{ij} are drawn i.i.d from Gaussian with mean zero and standard deviation σ . We use two different values for σ in our experiments: $\sigma = 0.05$ and $\sigma = 0.10$. For each σ , we note the following ratios:

$$\text{Noise-to-signal energy ratio} = \|\mathbf{N}\|_F / \|\mathbf{D}\|_F,$$

$$\text{Spectral ratio} = \|\mathbf{N}\|_2 / \sigma_k(\mathbf{D}),$$

where $\sigma_k(\mathbf{D})$ is the k -th largest singular value of \mathbf{D} . For $\sigma = 0.05$ and $\sigma = 0.10$, average Noise-to-signal energy ratio are 0.44 and 0.88, average Spectral ratio are 0.09 and 0.17, and average maximum absolute values of noise turn out to be 0.25 and 0.50, respectively. We denote noisy data by $\mathbf{A}_{0.05}$ (respectively $\mathbf{A}_{0.1}$) when \mathbf{D} is perturbed by \mathbf{N} whose elements \mathbf{N}_{ij} are drawn i.i.d from a Gaussian distribution with mean zero and $\sigma = 0.05$ (respectively $\sigma = 0.1$).

5.3.2 TechTC Datasets

These datasets (Gabrilovich and Markovitch (2004)) are bag-of-words features for document-term data describing two topics (ids). We choose four such datasets: TechTC1 with ids 10567 and 11346, TechTC2 with ids 10567 and 12121, TechTC3 with ids 11498 and 14517, TechTC4 with ids 11346 and 22294. Rows represent documents and columns are the words. We preprocessed the data by removing all the words of length four or smaller, and then normalized the rows by dividing each row by its Frobenius norm. The following table lists the dimension of the TechTC datasets.

Dimension ($m \times n$)	m	n
TechTC1	139	15170
TechTC2	138	11859
TechTC3	125	15485
TechTC4	125	14392

Table 1: Dimension of TechTC datasets

5.3.3 Handwritten Digit Data

A dataset (Hull (1994)) of three handwritten digits: six (664 samples), nine (644 samples), and one (1005 samples). Pixels are treated as features, and pixel values are normalized in $[-1,1]$. Each 16×16 digit image is first represented by a column vector by appending the pixels column-wise. Then, we use the transpose of this column vector to form a row in the data matrix. The number of rows $m = 2313$, and columns $n = 256$.

5.3.4 Stock Data

We use a stock market dataset (S&P) containing prices of 1218 stocks collected between 1983 and 2011. This temporal dataset has 7056 snapshots of stock prices. Thus, we have $m = 1218$ and $n = 7056$.

We provide summary statistics for all the datasets in Table 2. In order to compare our results with Achlioptas et al. (2013) we review the matrix metrics that they use. Let the numeric density of matrix \mathbf{X} be $\text{nd}(\mathbf{X}) = \|\mathbf{X}\|_1^2 / \|\mathbf{X}\|_F^2$. Clearly, $\text{nd}(\mathbf{X}) \leq \|\mathbf{X}\|_0$, with equality holding for zero-one matrices. The row density skew of \mathbf{X} is defined as

$$\text{rs}_0(\mathbf{X}) = \frac{\max_i \|\mathbf{X}_{(i)}\|_0}{\|\mathbf{X}\|_0 / m},$$

i.e., the ratio between number of non-zeros in the densest row and the average number of non-zeros per row. The numeric row density skew,

$$\text{rs}_1(\mathbf{X}) = \frac{\max_i \|\mathbf{X}_{(i)}\|_1}{\|\mathbf{X}\|_1 / m},$$

is a smooth analog of $\text{rs}_0(\mathbf{X})$. Achlioptas et al. (2013) assumed that $m \leq n$ without loss of generality, and for simplicity, $\max_i \|\mathbf{X}_{(i)}\|_\xi \geq \max_i \|\mathbf{X}^{(i)}\|_\xi$, for all $\xi \in \{0, 1, 2\}$. We notice that, although the Digit dataset does not satisfy the above conditions, its transpose does. We can work on the transposed dataset without loss of generality, and hence we take note of rs_0 and rs_1 of the transposed Digit data.

5.4 Results

We report all the results based on an average of five independent trials. We observe a small variance of the results.

5.4.1 Quality of Sparse Sketch

We first note that three sampling methods ℓ_1 , ℓ_2 , and hybrid- (ℓ_1, ℓ_2) , perform identically on noiseless data \mathbf{D} . We report the total probability of sampling noisy elements in $\mathbf{A} = \mathbf{D} + \mathbf{N}$ (elements which are zeros in \mathbf{D}). ℓ_1 sampling shows the highest susceptibility to noise, whereas, small-valued noisy elements are

	$\ \mathbf{X}\ _0$	nd	rs ₀	rs ₁
$\mathbf{A}_{0.05}$	2.5e+5	4.4e+4	1	2.66
$\mathbf{A}_{0.10}$	2.5e+5	9.2e+4	1	1.95
TechTC1	37831	12204	5.14	2.18
TechTC2	29334	9299	3.60	2.10
TechTC3	47304	14201	7.23	2.31
TechTC4	35018	10252	4.99	2.25
Digit	5.9e+5	5.1e+5	1	1.3
Stock	5.5e+6	6.5e+3	1.56	1.1e+03

Table 2: Summary statistics for the data sets

suppressed in ℓ_2 . Hybrid- (ℓ_1, ℓ_2) sampling, with $\alpha < 1$, samples mostly from true data elements, and thus captures the low-rank structure of the data better than ℓ_1 . The optimal mixing parameter α^* maintains the right balance between ℓ_2 sampling and ℓ_1 regularization and gives the smallest sample size to achieve a desired accuracy. Table 3 summarizes α^* for various data sets. Achlioptas et al. (2013) argued that, as long as $rs_0(\mathbf{X}) \geq rs_1(\mathbf{X})$, ℓ_1 sampling is better than ℓ_2 (even with truncation). Our results on α^* in Table 3 confirm this condition. Moreover, our method can derive the right blend of ℓ_1 and ℓ_2 sampling even when the above condition fails. In this sense, we generalize the results of Achlioptas et al. (2013).

	$\epsilon = 0.05$	$\epsilon = 0.75$	$rs_0 \geq rs_1$
$\mathbf{A}_{0.05}$	0.62	0.69	no
$\mathbf{A}_{0.1}$	0.63	0.70	no
TechTC1	1	1	yes
TechTC2	1	1	yes
TechTC3	1	1	yes
TechTC4	1	1	yes
Digit	0.20	0.74	no
Stock	0.74	0.75	no

Table 3: α^* for various data sets (ϵ is the desired relative-error accuracy). The last column compares α^* with the condition established by Achlioptas et al. (2013). Whenever $rs_0 \geq rs_1$, Achlioptas et al. (2013) show that ℓ_1 sampling is always better than ℓ_2 sampling, and we find $\alpha^* = 1$ (ℓ_1 sampling). However, when $rs_0 < rs_1$, $\alpha^* < 1$ and our hybrid sampling is strictly better.

Figure 4 plots $\mathcal{E} = \|\mathbf{A} - \tilde{\mathbf{A}}\|_2 / \|\mathbf{A}\|_2$ for various values of α and sample size s for various datasets. It clearly shows our optimal hybrid sampling is superior to ℓ_1 or ℓ_2 sampling.

We also compare the quality of sparse sketches produced via our hybrid sampling with that of ℓ_2 sampling with truncation. We use two predetermined truncation parameters, $\epsilon = 0.1$ and $\epsilon = 0.01$, for ℓ_2 sampling. First, ℓ_2 sampling without truncation turns out to be the worst for all datasets. ℓ_2 with $\epsilon = 0.01$ appears to produce sparse sketch $\tilde{\mathbf{A}}$ that is as bad as ℓ_2 without truncation for $\mathbf{A}_{0.1}$ and $\mathbf{A}_{0.05}$. However, ℓ_2 with $\epsilon = 0.1$ shows better performance than hybrid sampling, for $\mathbf{A}_{0.1}$ and $\mathbf{A}_{0.05}$, because this choice of ϵ turns out to be an appropriate threshold to zero-out most of the noisy elements. We must point out that, in this example, we control the noise, and we know what a good threshold may look like. However, in reality we have no control over the noise. Therefore, choosing the right threshold for ℓ_2 , without any prior knowledge, is an improbable task. For real datasets, it turns out that hybrid- (ℓ_1, ℓ_2) -hybrid sampling

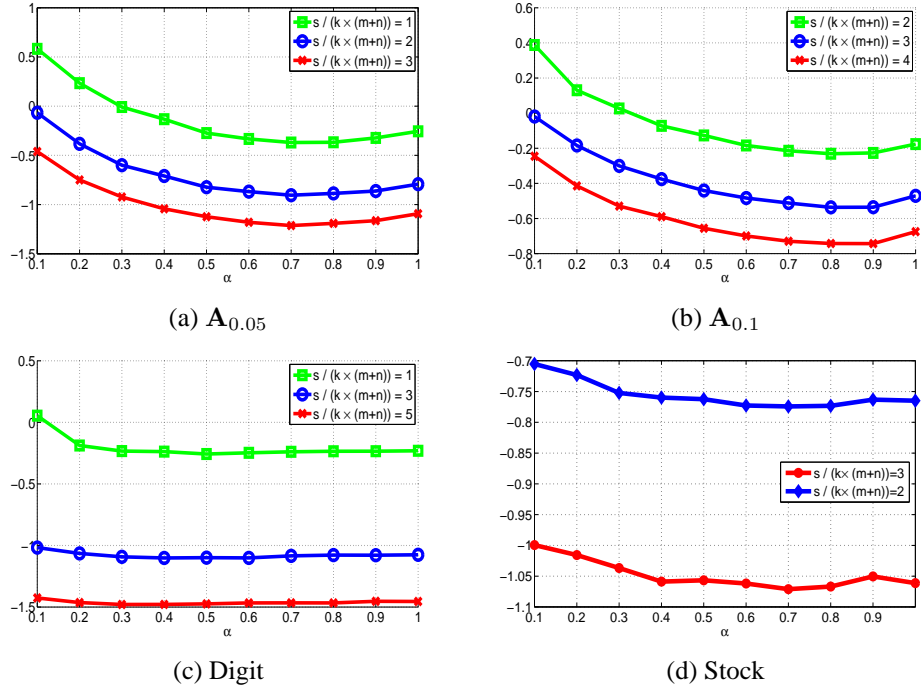


Figure 4: Approximation quality of sparse sketch $\tilde{\mathbf{A}}$: hybrid- (ℓ_1, ℓ_2) sampling, for various α and different sample size s , are shown. x -axis is α , and y -axis plots $\|\mathbf{A} - \tilde{\mathbf{A}}\|_2 / \|\mathbf{A}\|_2$ (in log₂ scale such that larger negative values indicate better quality). Each figure corresponds to a dataset: (a) $\mathbf{A}_{0.05}$, (b) $\mathbf{A}_{0.1}$, (c) Digit, and (d) Stock. We set $k = 5$ for synthetic data, $k = 3$ for Digit data, and $k = 1$ for Stock data. Choice of k is close to the stable rank of the data.

using α^* outperforms ℓ_2 sampling with the predefined thresholds for various sample sizes.

We compare the quality of Algorithm 3 producing an iterative estimate of α^* in a very restricted set up, i.e., one pass over the elements of data using $O(s)$ memory. Table 4 lists $\tilde{\alpha}$, the estimated α^* , for some of the datasets, for two choices of s using 10 iterations. We compare these values with the plots in Figure 4 where the results are generated without any restriction of size of memory or number of pass over the elements of the datasets.

	$\frac{s}{k \cdot (m+n)} = 2$	$\frac{s}{k \cdot (m+n)} = 3$
$\mathbf{A}_{0.05}, k = 5$	0.54	0.48
$\mathbf{A}_{0.1}, k = 5$	0.55	0.5
Digit, $k = 3$	0.69	0.89
Stock, $k = 1$	1	1

Table 4: Values of $\tilde{\alpha}$ (estimated α^* using Algorithm 3) for various data sets using one pass over the elements of data and $O(s)$ memory. We use $\epsilon = 0.05$, $\delta = 0.1$.

Finally, we compare our hybrid- (ℓ_1, ℓ_2) sampling with *element-wise leverage score* sampling (similar to Chen et al. (2014)) to produce quality sparse sketches from low-rank matrices. For this, we construct a 500×500 low-rank *power-law* matrix, similar to Chen et al. (2014), as follows: $\mathbf{A}_{pow} = \mathbf{D}\mathbf{X}\mathbf{Y}^T\mathbf{D}$, where, matrices \mathbf{X} and \mathbf{Y} are 500×5 i.i.d. Gaussian $\mathcal{N}(0, 1)$ and \mathbf{D} is a diagonal matrix with power-law decay, $\mathbf{D}_{ii} = i^{-\gamma}$, $1 \leq i \leq 500$. The parameter γ controls the ‘incoherence’ of the matrix, i.e., larger

values of γ makes the data more ‘spiky’. Table 5 lists the quality of sparse sketches produced via the two sampling methods.

	$\frac{s}{k(m+n)}$	hybrid- (ℓ_1, ℓ_2)	p_{lev}
$\gamma = 0.5$	3	42%	58%
	5	31%	43%
$\gamma = 0.8$	3	15%	43%
	5	12%	40%
$\gamma = 1.0$	3	8%	42%
	5	6%	39%

Table 5: Sparsification quality $\|\mathbf{A}_{pow} - \tilde{\mathbf{A}}_{pow}\|_2 / \|\mathbf{A}_{pow}\|_2$ for low-rank ‘power-law’ matrix \mathbf{A}_{pow} ($k = 5$). We compare the quality of hybrid- (ℓ_1, ℓ_2) sampling and leverage score sampling for two sample sizes. We note (average) α^* of hybrid- (ℓ_1, ℓ_2) distribution for data \mathbf{A}_{pow} using $\epsilon = 0.05, \delta = 0.1$. For $\gamma = 0.5, 0.8, 1.0$, we have $\alpha^* = 0.11, 0.72, 0.8$, respectively.

We note that, with increasing γ leverage scores get more aligned with the structure of the data, resulting in gradually improving approximation quality, for the same sample size. Larger γ produces more variance in data elements. ℓ_2 component of our hybrid distribution bias us towards the larger data elements, while ℓ_1 works as a regularizer to maintain the variance of the sampled (and rescaled) elements. With increasing γ we need more regularization to counter the problem of rescaling. Interestingly, our optimal parameter α^* adapts itself with this changing structure of data, e.g. for $\gamma = 0.5, 0.8, 1.0$, we have $\alpha^* = 0.11, 0.72, 0.8$, respectively. This shows the benefit of our parameterized hybrid distribution to achieve a superior approximation quality. Figure 5 shows the structure of the data \mathbf{A}_{pow} for $\gamma = 1.0$ along with the optimal hybrid- (ℓ_1, ℓ_2) distribution and leverage score distribution p_{lev} . The figure suggests our optimal hybrid distribution is better aligned with the structure of the data, requiring smaller sample size to achieve a desired sparsification accuracy.

We also compare the performance of the two sampling methods, optimal hybrid and leverage scores, on rank-truncated Digit data. It turns out that projection of Digit data onto top three principal components preserve the separation of digit categories. Therefore, we rank-truncate Digit data via SVD using rank three. Table 6 shows the superior quality of sparse sketches produced via optimal hybrid- (ℓ_1, ℓ_2) sampling for this rank-truncated digit data.

	Hybrid- (ℓ_1, ℓ_2)	p_{lev}
$\frac{s}{k(m+n)} = 3$	44%	61%
$\frac{s}{k(m+n)} = 5$	34%	47%

Table 6: Sparsification quality $\|\mathbf{A} - \tilde{\mathbf{A}}\|_2 / \|\mathbf{A}\|_2$ for rank-truncated Digit matrix ($k = 3$). We compare the optimal hybrid- (ℓ_1, ℓ_2) sampling and leverage score sampling for two sample sizes.

Finally, Table 7 shows the superiority of optimal hybrid- (ℓ_1, ℓ_2) sampling for rank-truncated (rank 5) $\mathbf{A}_{0.1}$ matrix for matrix sparsification.

5.4.2 Quality of Fast PCA

We investigate the quality of fast PCA approximation (Algorithm 4) for Digit data and $\mathbf{A}_{0.1}$. We set $r = 30 \cdot k$ for the random projection matrix \mathbf{A}_G to achieve a comparable runtime of \mathcal{G} with \mathcal{H} . Figure 6a

	Hybrid- (ℓ_1, ℓ_2)	p_{lev}
$\frac{s}{k(m+n)} = 3$	25%	80%
$\frac{s}{k(m+n)} = 5$	21%	62%

Table 7: Sparsification quality $\|\mathbf{A} - \tilde{\mathbf{A}}\|_2 / \|\mathbf{A}\|_2$ for rank-truncated $\mathbf{A}_{0.1}$ matrix ($k = 5$). We compare the optimal hybrid- (ℓ_1, ℓ_2) sampling and leverage score sampling using two sample sizes.

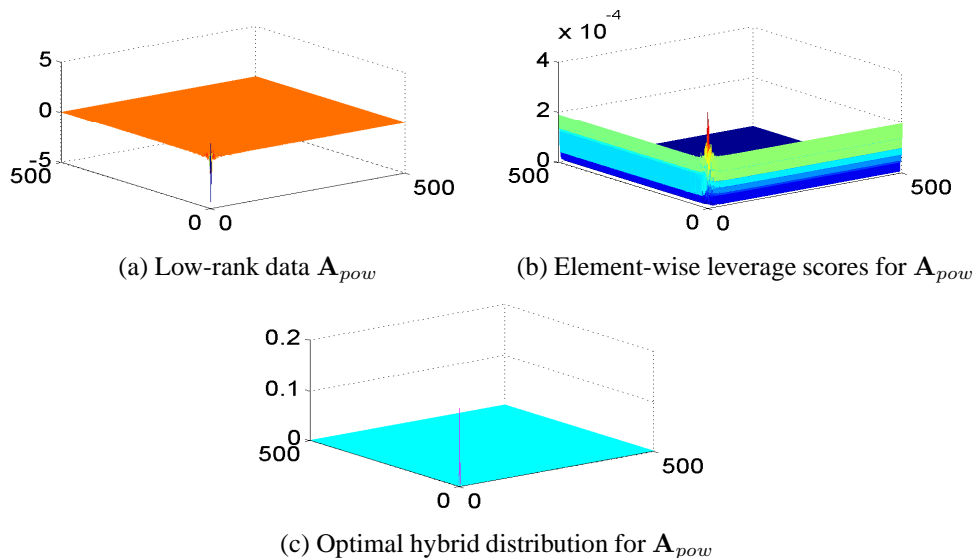


Figure 5: Comparing optimal hybrid- (ℓ_1, ℓ_2) distribution with leverage scores p_{lev} for data \mathbf{A}_{pow} for $\gamma = 1.0$. (a) Structure of \mathbf{A}_{pow} , (b) distribution p_{lev} , (c) optimal hybrid- (ℓ_1, ℓ_2) distribution. Our optimal hybrid distribution is more aligned with the structure of the data, requiring much smaller sample size to achieve a given accuracy of sparsification. This is supported by Table 5.

shows the PCA (exact and approximate) for Digit data. Also, we consider visualization of the projected data onto top three principal components (exact and approximate) in Figure 6b. In Figure 6b, we form an average digit for each digit category by taking the average of pixel intensities in the projected data over all the digit samples in each category. Similarly, Figure 7 shows the visual results for data $\mathbf{A}_{0.1}$ (we set $k = 5$). Finally, Table 8 lists the gain in computation time for Algorithm 4 due to sparsification.

	Sparsified Digit	Sparsified $\mathbf{A}_{0.1}$
Sparsity	93%	94%
$T_h/T_a/T_G$	30/151/36	18/73/36

Table 8: Computational gain of Algorithm 4 comparing to exact PCA. We report the computation time of MATLAB function ‘svds(\mathbf{A}, k)’ for actual data (T_a), sparsified data (T_h), and random projection data \mathbf{A}_G (T_G). We use only 7% and 6% of all the elements of Digit data and $\mathbf{A}_{0.1}$, respectively, to construct respective sparse sketches.

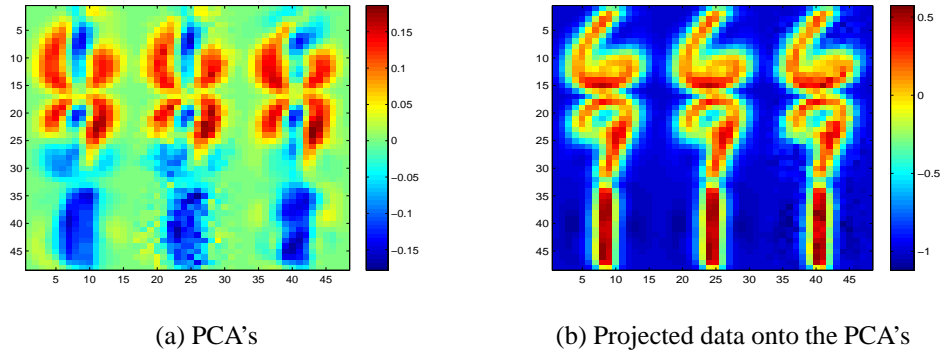


Figure 6: Approximation quality of fast PCA (Algorithm 4) on Digit data. (a) Visualization of principal components as 16×16 image. Principal components are ordered from the top row to the bottom. First column of PCA's are exact \mathcal{A} . Second column of PCA's are \mathcal{H} computed on sparsified data using $\sim 7\%$ of all the elements via optimal hybrid sampling. Third column of PCA's are \mathcal{G} computed on \mathbf{A}_G . Visually, \mathcal{H} is closer to \mathcal{A} . (b) Visualization of projected data onto top three PCA's. First column shows the average digits of projected actual data onto the exact PCA's \mathcal{A} . Second column is the average digits of projected actual data onto approximate PCA's (of sampled data) \mathcal{H} . We observe a similar quality of average digits of projected actual data onto approximate PCA's \mathcal{G} of \mathbf{A}_G . Third column shows the average digits for projected sparsified data onto approximate PCA's \mathcal{H} .

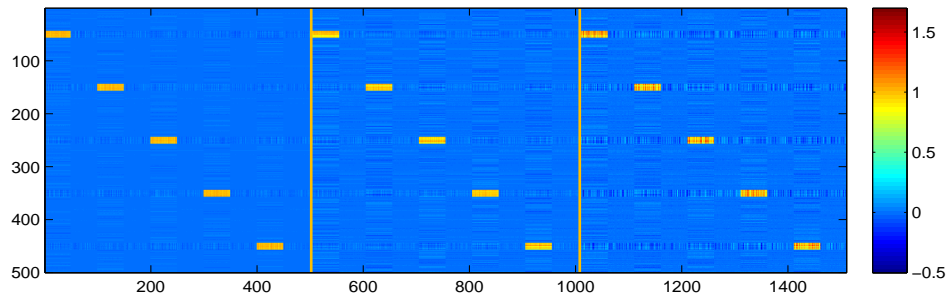


Figure 7: Approximation quality of fast PCA (Algorithm 4) for data $\mathbf{A}_{0.1}$. Visualization of projected data onto top five PCA's. Left image shows the projected actual data onto the exact PCAs \mathcal{A} . Middle image is the projection of actual data onto approximate PCA's (of sampled data) \mathcal{H} . We observe a similar quality of PCA's \mathcal{G} for \mathbf{A}_G . Right image shows the projected sparsified data onto approximate PCA's \mathcal{H} . We use only 6% of all the elements to produce the sparse sketches via optimal hybrid sampling.

5.5 Conclusion

Overall, the experimental results demonstrate the quality of the algorithms presented here, indicating the superiority of our approach to other extreme choices of element-wise sampling methods, such as, ℓ_1 and ℓ_2 sampling. Also, we demonstrate the theoretical and practical usefulness of hybrid- (ℓ_1, ℓ_2) sampling for fundamental data analysis tasks such as fast computation of PCA. Finally, our method outperforms element-wise leverage scores for the sparsification of various *low-rank* synthetic and real data matrices.

References

- D. Achlioptas and F. McSherry. Fast computation of low rank matrix approximations. In *Proceedings of Symposium on the Theory of Computing*, pages 611–618, 2001.
- D. Achlioptas and F. McSherry. Fast computation of low-rank matrix approximations. *Journal of the ACM*, page 54(2):9, 2007.
- D. Achlioptas, Z. Karnin, and E. Liberty. Matrix entry-wise sampling: Simple is best. In <http://citeseerx.ist.psu.edu/viewdoc/download?doi=10.1.1.297.576&rep=rep1&type=pdf>, 2013.
- S. Arora, E. Hazan, and S. Kale. A Fast Random Sampling Algorithm for Sparsifying Matrices. In *Approximation, Randomization, and Combinatorial Optimization. Algorithms and Techniques*, pages 272–279, vol 4110. Springer, 2006.
- Y Chen, S Bhojanapalli, S Sanghavi, and R Ward. Coherent Matrix Completion. *Proceedings of International Conference on Machine Learning*, pages 674–682, 2014.
- P. Drineas and A. Zouzias. A note on element-wise matrix sparsification via a matrix-valued Bernstein inequality. In *Information Processing Letters*, pages 385–389, 111(8), 2011.
- P. Drineas, R. Kannan, and M. W. Mahoney. Fast monte carlo algorithms for matrices I: approximating matrix multiplication. In *SIAM Journal on Computing*, pages 132–157, 36(1), 2006.
- E. Gabrilovich and S. Markovitch. Text categorization with many redundant features: using aggressive feature selection to make SVMs competitive with C4.5. In *Proceedings of International Conference on Machine Learning*, 2004.
- J. J. Hull. A database for handwritten text recognition research. In *IEEE Transactions on Pattern Analysis and Machine Intelligence*, pages 550–554, 16(5), 1994.
- A. Kundu and P. Drineas. A Note on Randomized Element-wise Matrix Sparsification. In <http://arxiv.org/pdf/1404.0320v1.pdf>, 2014.
- B. Recht. A simpler approach to matrix completion. In *The Journal of Machine Learning Research*, pages 3413–3430, 12, 2011.

This figure "Synthetic_k_5_data_mesh_noisy10.png" is available in "png" format from

<http://arxiv.org/ps/1503.00547v1>